

ARTICLES

Critical Dynamics of the Binary System Nitroethane/3-Methylpentane: Relaxation Rate and Scaling Function

I. Iwanowski, K. Leluk,[†] M. Rudowski,[†] and U. Kaatz*^{*}*Drittes Physikalisches Institut, Georg-August-Universität, Friedrich-Hund-Platz 1, 37077 Göttingen, Germany**Received: November 30, 2005*

Shear viscosity and dynamic light scattering measurements as well as ultrasonic spectrometry studies of the nitroethane/3-methylpentane mixture of critical composition have been performed at various temperatures near the critical temperature, T_c . A combined evaluation of the shear viscosity and mutual diffusion coefficient data yielded the amplitude, ξ_0 , of the fluctuation correlation length, ξ , assumed to follow power law, and the relaxation rate, Γ , or order parameter fluctuations. The latter was found to follow power law with the theoretical universal exponent. The amplitudes $\xi_0 = 0.23 \pm 0.02$ nm and $\Gamma_0 = (125 \pm 5) \times 10^9$ s⁻¹ nicely agree with literature values. Using the relaxation rates resulting from the viscosity and diffusion coefficient data, the scaling function has been calculated assuming the ultrasonic spectra to be composed of a critical part and a noncritical background contribution. The experimental scaling function fits well to the predictions of the Bhattacharjee–Ferrell dynamic scaling model with scaled half-attenuation frequency, $\Omega_{1/2}^{\text{BF}} = 2.1$. The amplitude of the sonic spectra yields the amount $|g| = 0.26$ of the adiabatic coupling constant, g , in fair agreement with -0.29 from another thermodynamic relation.

1. Introduction

A fascinating feature of systems near a critical point is their ability to display fluctuations of vast sizes. Individual properties are masked thereby so that the critical behavior can be well represented by universal laws.^{1–4} The critical dynamics of binary liquids near their consolute point is governed by the dynamic scaling hypothesis^{5–8}

$$\Gamma = 2D/\xi^2 \quad (1)$$

Equation 1 is based on the idea that fluctuations in the local mixture composition follow a diffusion law. It relates the relaxation rate, Γ , of order parameter fluctuations to the fluctuation correlation length, ξ , and the mutual diffusion coefficient, D . Close to a critical point, the fluctuation correlation length increases. Simultaneously, the mutual diffusion coefficient becomes smaller. As a consequence, the relaxation rate, Γ , of a mixture critical composition decreases significantly when the system approaches the critical temperature, T_c . This phenomenon is well-known as “critical slowing down” of the microdynamics of the liquid.

Normally, the relaxation rate follows power law

$$\Gamma(\epsilon) = \Gamma_0 \epsilon^{Z_0 \nu} \quad (2)$$

In this relation, $\epsilon (=|T - T_c|/T_c)$ denotes the reduced temperature, Γ_0 is an amplitude, and Z_0 and ν are universal critical exponents. The value for the dynamical critical exponent follows

as $Z_0 = 3.065$ from renormalization group theory.¹ The value for the critical exponent of the fluctuation correlation length is $\nu = 0.63$.¹

The dynamic scaling hypothesis can be verified or disproved by ultrasonic attenuation spectrometry, yielding Γ , as well as dynamic light scattering and shear viscosity measurements, from which D and ξ can be derived. Unfortunately, the evaluation of experimental data in terms of these quantities does not necessarily lead to as clear conclusions as required for a strict investigation of eq 1. Various theoretical models exist. Among those describing the ultrasonic spectra of critical systems, we mention the dynamic scaling theory,^{9–11} the mode–mode coupling theory,^{12–14} and the more recent theory that proceeds from an intuitive description of the bulk viscosity near the critical point,^{15,16} and it is not evident presently which model applies better to the experimental findings. The situation is even more complicated because measurements normally extend to regimes less close to the critical point, so that effects from the crossover from Ising to mean-field behavior may act as an influence on the data. Another significant point is the fact that, with many critical systems of interest, the fluctuations in the local composition seem to couple to other elementary molecular processes, such as the dimerization of carboxylic acids,¹⁷ the monomer exchange between micelles and the suspending phase,¹⁸ and the rotational diffusion of membrane molecules in phospholipid bilayers.¹⁹ Liquids exhibiting such coupling phenomena are, of course, less suited for an examination of the scaling hypothesis. They are, however, valuable systems to study the influence of the basically universal critical fluctuations upon the individual molecular processes and vice versa, provided

* Corresponding author. E-mail: uka@physik3.gwdg.de.

[†] Permanent address: Faculty of Chemistry, University of Wrocław, 14, F. Joliot-Curie, 50-383 Wrocław, Poland.

the critical behavior and scaling properties of simpler mixtures without crossover to other elementary processes are sufficiently well-known.

In this situation, we found it interesting to perform an investigation into the critical dynamics of the system nitroethane/3-methylpentane (NE/3-MP). Ultrasonic spectra of the NE/3-MP mixture of critical composition are expected to not contain contributions from elementary molecular processes with relaxation characteristics, in addition to the concentration fluctuations. This feature facilitates a rigorous evaluation of the experimental spectra in terms of the critical dynamics. Ultrasonic attenuation measurements of the NE/3-MP system have indeed been used previously to determine the relaxation rate of order parameter fluctuations.²⁰ In that study, however, the agreement of the attenuation data with the theoretical form of the scaling function was imperfect and no shear viscosity and dynamic light scattering data were available for comparison. Ultrasonic attenuation data have also been reported for NE/3-MP mixtures of noncritical composition, and a pseudospinodal conception has been applied to discuss their scaling behavior.²¹ Again, no independent methods were included for a determination of the relaxation rate.

A noteworthy favorable feature of the NE/3-MP mixture of critical composition is its close relation to the nitroethane/cyclohexane (NE/CH) critical system. The latter has been intensively studied recently²² so that the results for both binary mixtures with many similar properties can be compared to one another.

2. Experimental Section

Samples. Nitroethane (NE, $\geq 99.5\%$) and 3-methylpentane (3-MP, $\geq 99\%$) were purchased from Aldrich and have been used as delivered by the manufacturers. To avoid uptake of water from the air, all samples have been prepared and always kept under dry nitrogen. The NE/3-MP system exhibits an upper critical demixing point at equimolar composition (mole fraction $X = 0.500 \pm 0.001$,^{23–27} mass fraction of nitroethane $Y_{\text{NE}} = 0.466$). The visually determined phase separation temperature of the mixture of critical composition ($X = 0.500$) was 299.68 ± 0.05 K, slightly higher than the critical temperatures, T_c , given in the literature: 299.61 ,²³ 299.60 ,^{20,23,25} 299.58 ,²⁰ 299.57 ,²⁴ 299.55 ,²⁶ and 299.09 K.²⁷

Measurements. The shear viscosity, η_s , of the NE/3-MP mixture of critical composition has been measured as a function of temperature, T , using Ubbelohde-type capillary viscosimeters (Schott, Mainz, Germany) and a falling ball viscosimeter (Haake, Karlsruhe, Germany). Both instruments had been calibrated against deionized, distilled, and carefully degassed water. For the capillary viscosimeters, shear rates can be defined. It was found, however, that corrections in the experimental η_s data for the finite shear rate^{28–30} were negligibly small. Since, in the falling ball viscosimeter measurements, the sample is contained in a sealed volume, this method effectively reduces the risk of changes in the composition of the critical mixture, as may result from preferential evaporation in the experiments with open capillaries. We therefore used the η_s data from the falling ball measurements only. The experimental error in the viscosity data was $\Delta\eta_s/\eta_s = 0.03$. Temperature fluctuations during the measurements were smaller than ± 0.02 K.

The mutual diffusion coefficient, $D(T)$, of the NE/3-MP mixture of critical composition has been determined from the decay rate, $\Gamma_1(q, T)$, of the normalized autocorrelation function

$$S_1(q, t) = \exp[-t\Gamma_1(q, T)] \quad (3)$$

of the light quasielastically scattered from the sample using the relation

$$D = \Gamma_1(q, T)/q^2 \quad (4)$$

Here, q is the amount of the wavevector \vec{q} selected by the scattering geometry

$$q = \frac{4\pi n}{\lambda_0} \sin(\theta/2) \quad (5)$$

where n denotes the optical refractive index of the liquid, λ_0 is the wavelength of the incident light, and θ is the scattering angle. We applied a self-beating digital photon correlation spectrometer³¹ to determine S_1 . The spectrometer was provided with a goniometer system and with a special planar-window cell to allow for variations of \vec{q} .³² To avoid problems from a width, θ , varying scattering volume, data at $\theta = \pi/2$ have been finally used. We used a frequency-doubled Nd:YAG laser ($\lambda_0 = 532$ nm, Coherent, Santa Clara, CA) as the light source and analyzed the scattered board in a real-time mode of operation with the aid of a digital correlator board (ALV-500/E, Laser, Langen, Germany). It enables correlation function measurements within a time scale from 2×10^{-7} to 3.4×10^3 s.^{33,34} The refractive index, n , of the sample has been measured with a refractometer (Zeiss, Obercochem, Germany). The experimental error in the diffusion coefficient data was $\Delta D/D = 0.05$. During the light scattering experiments, the temperature of the sample was controlled to within 0.02 K and was measured with an error less than 0.01 K.

Acoustical attenuation coefficient measurements for the determination of the scaling function in the ultrasonic spectra covered the frequency range from 200 kHz to 1.7 MHz. A resonator method has been applied in which the path length of interaction of the ultrasonic waves with the sample is essentially enhanced by multiple reflections.³⁵ The focusing action of a cavity resonator cell with a concavely shaped end face³⁶ was utilized in these measurements, because it reduces unwanted effects from mechanical stress at varying temperature. Using this resonator method, the attenuation coefficient, α , of the sample was determined relative to that of a reference liquid with matched sound velocity, c_s , and density, ρ .^{35,36} To carefully take into account effects from higher order modes of the cavity field, we always recorded, in a suitable frequency range around the principal resonance peak, the complete transfer function of the cell. The transfer function was subsequently fitted to appropriate analytical expressions in order to obtain the principle peak unaffected by higher modes. The temperature of the cavity resonator was controlled to within 0.03 K and measured with an error of less than 0.02 K. The frequency of measurement was known and kept constant with a negligibly small error. The error in the attenuation coefficients was less than $\Delta\alpha/\alpha = 0.05$.

At some temperatures, the ultrasonic spectra were complemented by absolute α measurements in the frequency range 10–430 MHz. A pulse-modulated wave transmission method at variable sample length was applied.³⁵ We used two cells, each matched to a particular frequency range. The transducers of the cells were operated at the odd overtones of their fundamental longitudinal frequency, ν_T . The cells mainly differed from one another by their dimensions and by their transmitter and receiver transducers ($\nu_T = 1$ MHz, quartz, frequency range of operation $10 \leq \nu \leq 170$ MHz;³⁷ $\nu_T = 10$ MHz, lithium niobate, $50 \leq \nu \leq 430$ MHz³⁸). To avoid errors from nonlinearities in the electronic setup, calibration procedures were routinely run in which the cells were substituted by high-precision below-cutoff

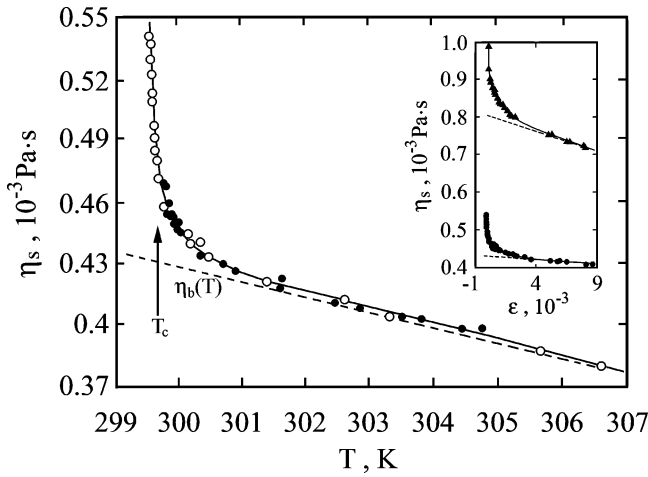


Figure 1. Shear viscosity, η_s , of the NE/3-MP mixture of critical composition displayed versus temperature, T . The circles represent data from the literature.²⁴ The full line is the graph of the theoretical shear viscosity relation (eqs 6–11), the dashed line shows the background contribution, η_b (eq 7), to η_s . In the inset, the shear viscosity data of the NE/3-MP system (points) are given along with those for the NE/CH mixture of critical composition (triangles²²).

piston attenuators.³⁹ With these cells, fluctuations in the sample temperature also did not exceed 0.03 K. Variations in the frequency, ν , of the measurement signal were again negligibly small. The error in the attenuation coefficient data was smaller than $\Delta\alpha/\alpha = 0.02$.

The sound velocity, c_s , of the mixture of critical composition followed with an error of less than $\Delta c_s/c_s = 0.005$ as a byproduct from the resonator measurements. The resonance frequencies of successive principal resonance peaks were evaluated for this purpose, carefully considering their nonequidistant distribution.³⁶

3. Results and Discussion

Shear Viscosity and Diffusion Coefficient. Along with literature data,²⁴ the shear viscosities, η_s , of the NE/3-MP mixture of critical composition, as obtained from the falling ball viscosimeter measurements, are displayed as a function of temperature, T , in Figure 1. Within the limits of experimental errors, the η_s data from both series of measurements fit to one another and also to the data of ref 40. The shear viscosity displays a background contribution, slowly decreasing with T and, close to T_c ($\epsilon \leq 5 \times 10^{-3}$), a singular part that distinctly increases when approaching T_c . In the inset of Figure 1, the shear viscosities of the NE/3-MP mixture are compared to those of the similar system nitroethane/cyclohexane (NE/CH, $T_c = 296.46$ K²²). The background contribution of the latter is much larger than that of the NE/3-MP mixture, thus reflecting the significantly different viscosities of the alkanes ($\eta_s = 0.437 \times 10^{-3}$ Pa·s, 3-MP, 25 °C; $\eta_s = 0.910 \times 10^{-3}$ Pa·s, CH, 25 °C).

To consider crossover corrections for the transition to the hydrodynamic regime, the shear viscosity has been treated in terms of the relation^{41–43}

$$\eta_s(\epsilon) = \eta_b(\epsilon) \exp(Z_\eta H) \quad (6)$$

with the background viscosity

$$\eta_b(\epsilon) = A_\eta \exp[B_\eta(T - T_\eta)] \quad (7)$$

In eq 7, A_η , B_η , and T_η are system specific parameters. In eq 6, Z_η is the universal critical exponent of viscosity ($Z_\eta = 0.065$ ^{28,29,41}) and H is given by

$$H = \frac{1}{12} \sin(3\psi_D) - \frac{1}{4q_D} \xi \sin(2\psi_D) + \frac{1}{(q_c \xi)^2} \left[1 - \frac{5}{4} (q_c \xi)^2 \sin \psi_D \right] - \frac{1}{(q_c \xi)^3} \left\{ \left[1 - \frac{3}{2} (q_c \xi)^2 \right] \psi_D - \left[(q_c \xi)^2 - 1 \right]^{3/2} L(\tilde{\omega}) \right\} \quad (8)$$

Herein, q_c and q_D are cutoff wavenumbers and

$$\psi_D = \arccos(1 + q_D^2 \xi^2)^{-1/2} \quad (9)$$

$$\tilde{\omega} = \left| \frac{q_c \xi - 1}{q_c \xi + 1} \right|^{1/2} \tan(\psi_D/2) \quad (10)$$

$$L\tilde{\omega} = \begin{cases} \ln\left(\frac{1 + \tilde{\omega}}{1 - \tilde{\omega}}\right), & \text{if } q_c \xi > 1 \\ 2 \arctan|\tilde{\omega}|, & \text{if } q_c \xi \leq 1 \end{cases} \quad (11)$$

The mutual diffusion coefficient, D , of the critical system is related to the shear viscosity. It is likewise given by two parts^{42,43}

$$D = \Delta D + D_b \quad (12)$$

with the singular part

$$\Delta D = D_{KF} R \Omega_K(x) (1 + b^2 x^2)^{Z_\eta/2} \quad (13)$$

the background part

$$D_b = D_{KF} \frac{3\pi\eta_s}{16\eta_b} (1 + x^2) \left(\frac{1}{q_D \xi} - \frac{1}{\tilde{q}_c \xi} \right) \quad (14)$$

and with the Stokes–Einstein–Kawasaki–Ferrell relation for the hydrodynamic limit^{7,44–46}

$$D_{KF} = \frac{k_B T}{6\pi\eta_s \xi} \quad (15)$$

In these relations, $R = 1.03$, $b = 0.55$, $x = q\xi$, with the amount q of the wave vector according to eq 5, and k_B denotes Boltzmann's constant. In eq 13, $\Omega_K(x)$ is the Kawasaki function, defined as⁴⁷

$$\Omega_K(x) = \frac{3}{4x^2} \left[1 + x^2 + \left(x^3 - \frac{1}{x} \right) \arctan x \right] \quad (16)$$

and in eq 14

$$\tilde{q}_c^{-1} = q_c^{-1} + (2q_D)^{-1} \quad (17)$$

Using power law behavior

$$\xi(\epsilon) = \xi_0 \epsilon^{-\bar{\nu}} \quad (18)$$

to represent the fluctuation correlation length in a combined regression analysis of the shear viscosity and light scattering data, the values presented in Table 1 for the six adjustable parameters ξ_0 , A_η , B_η , T_η , q_c , and q_D have been found. The temperature dependencies of η_s and D resulting from these parameters are displayed in Figures 1 and 2, respectively. Both functions are in fair agreement with the experimental results.

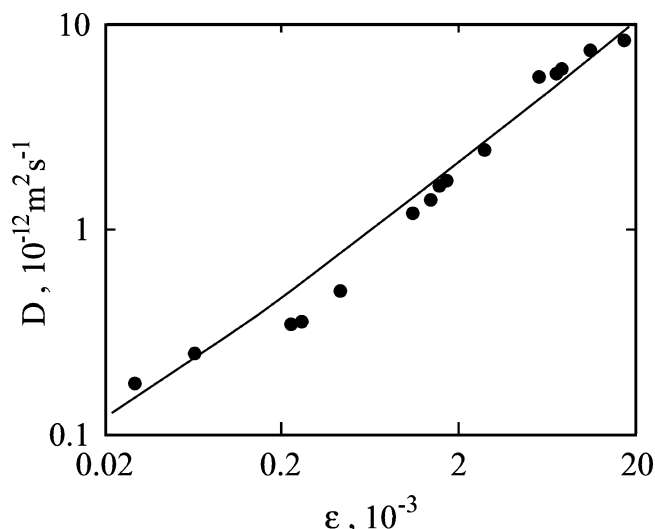


Figure 2. Mutual diffusion coefficient of the NE/3-MP mixture of critical composition versus reduced temperature. The line represents the theoretical diffusion coefficient relation (eqs 12–18).

TABLE 1: Parameters of the Shear Viscosity (eqs 6–11) and Diffusion Coefficient Relations (eqs 12–18) for the Nitroethane/3-Methylpentane and Nitroethane/Cyclohexane²² Mixtures of Critical Composition

	ξ_0 , nm ± 0.02	A_η , 10^6 Pa·s ± 0.02	B_η , K ± 200	T_η , K ± 20	q_c , 10^9 m ⁻¹	q_D , 10^9 m ⁻¹
NE/3-MP	0.23	0.23	2877	-84	1.3	0.32
NE/CH	0.16	0.55	2537	-51	≥ 1000	0.55

Use of the more recent crossover function,⁴⁸ H , in eq 6 does not noticeably change the relevant data derived from this analysis.

Fluctuation Correlation Length and Relaxation Rate. Also shown in Table 1 are literature data from combined evaluations of shear viscosity and dynamic light scattering measurements of the NE/3-MP mixture of critical composition⁴⁰ as well as for the similar system NE/CH.²² In the previous analysis of NE/3-MP, measurements⁴⁰ of the viscosity had been represented by an equation of the form^{42,49}

$$\eta_s(\epsilon) = \eta_b(\epsilon)(q_D \xi)^{Z_\eta} \quad (19)$$

assuming $T_\eta \equiv 0$ in the background part of the shear viscosity (eq 7). The parameters A_η and B_η from the two series of experimental data and different evaluation procedures agree with one another within the limits of experimental errors. The deviations in the amplitude of the fluctuation correlation length are supposed to be due to the insufficient consideration of crossover effects by relation 19 which had been derived for a temperature range close to the critical point only.^{41–43,50}

The amplitude, ξ_0 , of the NE/3-MP system is significantly larger than that of the NE/CH system (Table 1). This difference in the fluctuation correlation length of similar binary critical mixtures is obviously a reflection of their different shear viscosities. As mentioned before, the η_s value of NE/CH is substantially higher than that of NE/3-MP. Figure 3 roughly indicates an inverse relation between ξ_0 and the background viscosity at T_c of some binary critical mixtures.

Figure 4 shows the relaxation rate, $\Gamma(\epsilon)$, of order parameter fluctuations which according to eq 1 has been calculated from the mutual diffusion coefficient and the fluctuation correlation length. The Γ values follow power law (eq 2) with the theoretical exponent $Z_0 \bar{\nu}$. The amplitude, Γ_0 , results as $(125 \pm 5) \times 10^9$

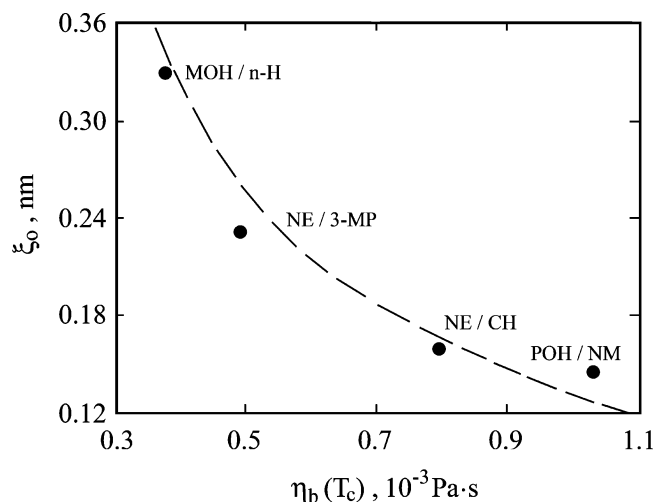


Figure 3. Amplitude, ξ_0 , of the fluctuation correlation length (eq 18) as a function of the background part, $\eta_b(T_c)$, in the shear viscosity at T_c : MOH/*n*-H, methanol/*n*-hexane;⁵³ NE/CH, nitroethane/cyclohexane;²² POH/NM, pentanol/nitromethane.⁵²

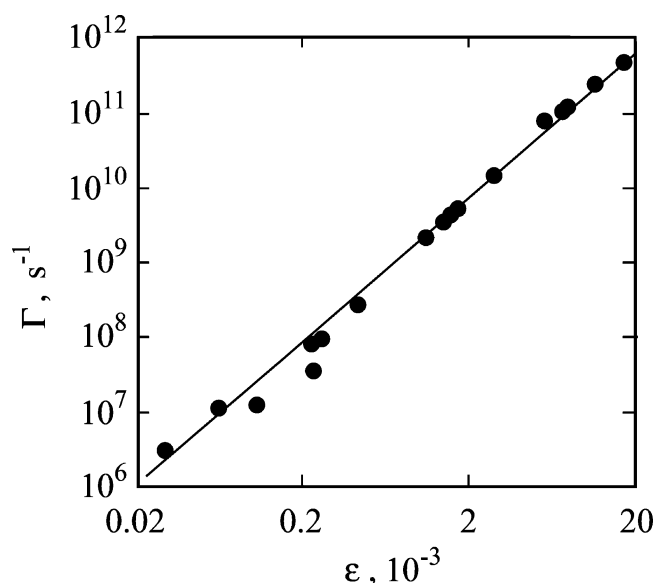


Figure 4. Relaxation rate, Γ , of order parameter fluctuations for the NE/3-MP mixture of critical composition displayed versus reduced temperature, ϵ . The line represents power law (eq 2) with the theoretical universal exponent and with the amplitude $\Gamma_0 = 125 \times 10^9$ s⁻¹.

s⁻¹ from our measurements. This value compares to the value $\Gamma_0 = 123 \times 10^9$ s⁻¹ that Garland and Sanchez obtained from their analysis of shear viscosity, Rayleigh line width, and photon correlation spectrometry data.²⁰

The Γ_0 value for the NE/3-MP mixture of critical composition is smaller than the amplitudes for the systems NE/CH ($\Gamma_0 = 156 \times 10^9$ s⁻¹)²² and nitromethane/*n*-pentanol ($\Gamma_0 = 187 \times 10^9$ s⁻¹)⁵², both exhibiting a smaller amplitude, ξ_0 , of the fluctuation correlation length (Figure 3). For most other binary liquids studied so far, the Γ_0 values are distinctly smaller, for example, $\Gamma_0 = 44 \times 10^9$ s⁻¹, methanol/*n*-hexane;⁵³ $\Gamma_0 = 26 \times 10^9$ s⁻¹, methanol/cyclohexane;⁵¹ $\Gamma_0 = 0.26 \times 10^9$ s⁻¹, ethylammonium nitrate/*n*-octanol.⁵⁴

Scaling Function and Adiabatic Coupling Constant. In the frequency range between 200 kHz and 300 MHz and ultrasonic attenuation spectrum close to T_c of the NE/3-MP mixture of critical composition is displayed in Figure 5. To accentuate the

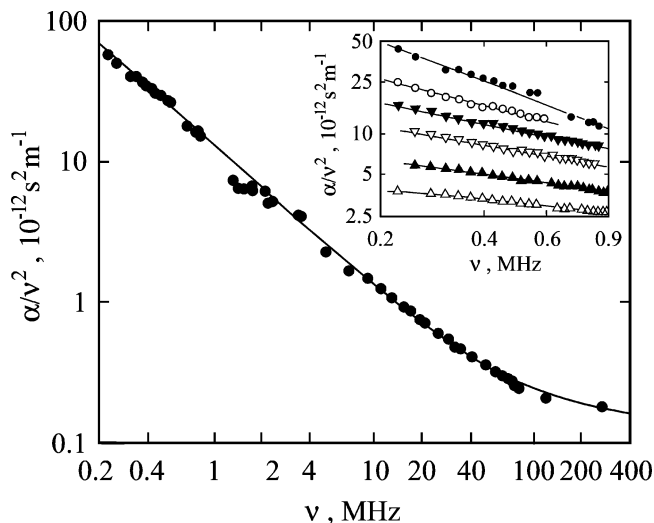


Figure 5. Ultrasonic attenuation spectra in the format α/ν^2 versus ν of the NE/3-MP mixture of critical composition at 300.05 K. The line is the graph of the relaxation spectral function (eqs 22–24) used to analytically represent the data. The inset shows the low-frequency part of the spectra at various distances, $\Delta T = T - T_c$, from the critical temperature: (Δ) $\Delta T = 4.15$ K; (\blacktriangle) $\Delta T = 3.19$ K; (∇) $\Delta T = 2.15$ K; (\blacktriangledown) $\Delta T = 1.73$ K; (\circ) $\Delta T = 1.29$ K; (\bullet) $\Delta T = 0$.

low-frequency part of the spectrum, the data are presented in the frequency normalized format

$$\alpha/\nu^2 = \alpha_\lambda/(\nu c_s) \quad (20)$$

Here, α is the sonic attenuation coefficient and $\alpha_\lambda = \alpha \cdot \lambda$ is the attenuation per wavelength, $\lambda = c_s/\nu$. Within the range of measurements, the α/ν^2 data decrease considerably with frequency and tend toward an asymptotically constant value

$$B'(T) = \lim_{\nu \rightarrow \infty} (\alpha/\nu^2) \quad (21)$$

at high frequencies.

In the inset of Figure 5, the low-frequency part of the α/ν^2 spectrum is shown at six temperatures above T_c . The data have been obtained from resonator measurements without refilling the cells between two runs. At a given frequency, the frequency dependent low-frequency data increase substantially when the temperature approaches T_c . These characteristics suggest the ultrasonic spectra of the NE/3-MP mixture to be composed of two parts

$$\alpha_\lambda(\nu, T) = \alpha_\lambda^c(\nu, T) + \alpha_\lambda^b(\nu, T) \quad (22)$$

of which α_λ^c represents the critical contribution, strongly dependent upon temperature near T_c , and α_λ^b represents the noncritical background contribution. There are no obvious indications of noncritical background contributions with relaxation characteristics within the frequency range of measurements. We are aware that such contributions, if their amplitude is sufficiently small, may be masked by the predominating critical part which extends over a broad frequency domain. We nevertheless assume the noncritical contribution to be simply given by the frequency independent B' value:

$$\alpha_\lambda^b(\nu, T) = B'(T) c_s(T) \nu = B(T) \nu \quad (23)$$

According to the Bhattacharjee–Ferrell dynamic scaling model,^{9,10}

the critical part in the attenuation coefficient per wavelength may be expressed as

$$\alpha_\lambda^c(\nu, T) = c_s(T) A(T) F(\Omega) \quad (24)$$

with the sound velocity, c_s , and the amplitude, A , weakly dependent upon frequency and temperature, T , and with the universal scaling function, F , that depends on the scaled frequency

$$\Omega = 2\pi\nu/\Gamma(\epsilon) \quad (25)$$

The scaling function

$$F(\Omega) = \frac{3}{\pi} \int_0^\infty \frac{\Omega x(1+x)^{1/2}}{x^2(1+x) + \Omega^2(1+x)^2} x dx \quad (26)$$

can be well represented by the empirical form¹⁰

$$F_{\text{BF}}(\Omega) = [1 + 0.414(\Omega_{1/2}^{\text{BF}}/\Omega)^{1/2}]^{-2} \quad (27)$$

Herein, $\Omega_{1/2}^{\text{BF}}$ denotes the scaled half-attenuation frequency of F_{BF} :

$$F_{\text{BF}}(\Omega_{1/2}^{\text{BF}}) = 0.5 \lim_{\Omega \rightarrow \infty} F_{\text{BF}}(\Omega) = 0.5 \quad (28)$$

Bhattacharjee and Ferrell have predicted $\Omega_{1/2}^{\text{BF}} = 2.1$ from theoretical arguments but have noted that the value of the half-attenuation frequency is not well defined from their model.¹⁰ Recent experimental findings verify the theoretically predicted $\Omega_{1/2}^{\text{BF}} = 2.1$ value^{22,51,53,55} even though the somewhat smaller value $\Omega_{1/2}^{\text{BF}} = 1.8 \pm 0.1$ has been found for the critical mixture *n*-pentanol/nitromethane.⁵² To reduce the number of unknown parameters, we thus analyzed the ultrasonic spectra of the NE/3-MP system using the empirical scaling function, $F_{\text{BF}}(\Omega)$, with a scaled half-attenuation frequency of $\Omega_{1/2}^{\text{BF}} = 2.1$.

Taking into account the weak dependence of the sound velocity, c_s , and the amplitude, A , of the critical term upon temperature, the scaling function can be calculated as the ratio^{10,22}

$$F(\Omega) = F^* \frac{\alpha_\lambda^c(\nu, T)}{\alpha_\lambda^c(\nu, T_c)} = F^* \frac{\alpha_\lambda(\nu, T) - \nu B(T)}{\alpha_\lambda(\nu, T_c) - \nu B(T_c)} \quad (29)$$

from experimental data. Here,

$$F^*(T) = \frac{c_s(T_c) A(T_c)}{c_s(T) A(T)} \quad (30)$$

Again, for simplicity, we have used $F^* \equiv 1$ as originally proposed by Bhattacharjee and Ferrell.¹⁰ The B values of the background part have been obtained from our broadband ultrasonic measurements as $B(T) = [102 - 0.1(T - 273.15\text{K})] \times 10^{-15}$ s. Using these B values and the relaxation rates, Γ , as resulting from the shear viscosity and quasielastic light scattering measurements, the scaling function can be calculated from the sonic attenuation coefficients without any adjustable parameter. The scaling function following from our T dependent low-frequency ultrasonic measurements is shown in Figure 6 where also data from the literature²⁰ are presented.

The experimental data nicely fit to the empirical scaling function $F_{\text{BF}}(\Omega)$, the graph of which is also given in Figure 6. In particular, at small scaled frequencies ($\Omega < 2$), the agreement between the experimental data and the theoretical predictions

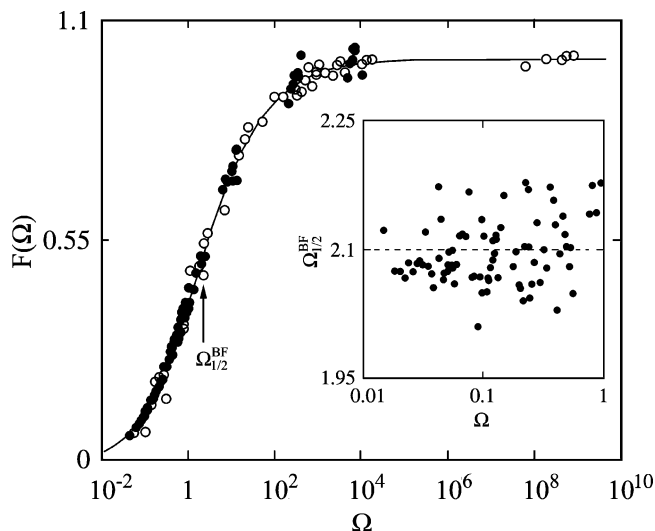


Figure 6. Scaling function data (eqs 29 and 30) versus reduced frequency, Ω , for the NE/3-MP mixture of critical composition. The circles represent data from the literature.²⁰ The line is the graph of the empirical scaling function, $F_{\text{BF}}(\Omega)$, defined by eq 27. For small reduced frequencies, the inset shows the scaled half-attenuation frequency, $\Omega_{1/2}^{\text{BF}}$, as according to⁵⁵ $\Omega_{1/2}^{\text{BF}} = \Omega[F(\Omega)/0.4142 - 1]^2$ following from the sonic attenuation coefficients.

is excellent, indicating that $\Omega_{1/2}^{\text{BF}}$ well applies to the system NE/3-MP. At scaled frequencies between 10^2 and 10^4 , data from the temperature runs exhibit some systematic deviations from the theoretical form of $F(\Omega)$. These small deviations may be due to the neglect of the slight temperature dependence in the factor F^{*22} and/or to a hidden low-amplitude noncritical relation term within the frequency range of measurements. The literature $F(\Omega)$ data²⁰ match with our data and complement them at very high reduced frequencies.

From the amplitude parameter, $A(T)$, of the critical part in the ultrasonic spectra, the amplitude

$$S(T) = A(T)\nu^\delta \quad (31)$$

of the dynamic scaling model¹⁰ can be derived which, according to

$$S(T) = \frac{\pi^2 \delta C_{\text{pc}} c_s(T_c)}{2T_c C_{\text{pb}}^2(T)} \left[\frac{\Omega_{1/2}^{\text{BF}} \Gamma_0}{2\pi} \right]^\delta g^2(T) \quad (32)$$

is related to the adiabatic coupling constant, g . Here, $\delta = \alpha_0/(Z_0 \tilde{\nu}) = 0.06$ is the universal critical exponent. C_{pc} and C_{pb} are the amplitude of the singular part and the background part of the specific heat, C_p , at constant pressure, assumed to be simply given by

$$C_p(\epsilon) = C_{\text{pc}} \epsilon^{\alpha_0} + C_{\text{pb}} \quad (33)$$

The Bhattacharjee–Ferrell amplitude follows as $S = (2.9 \pm 0.3) \times 10^{-5} \text{ s}^{0.94} \text{ m}^{-1}$ from our ultrasonic attenuation measurements, in nice agreement with the value $S = (3.04 \pm 0.1) \times 10^{-5} \text{ s}^{0.94} \text{ m}^{-1}$ obtained by Garland and Sanchez.²⁰ With $c_s(T_c) = 1098 \text{ ms}^{-1}$ (ref 20), $T_c = 299.68 \text{ K}$, $\Gamma_0 = 125 \times 10^9 \text{ s}^{-1}$, $\Omega_{1/2}^{\text{BF}} = 2.1$, and $C_{\text{pb}} = 1.71 \text{ J g}^{-1} \text{ K}^{-1}$ (ref 20) or $C_{\text{pb}} = 1.66 \text{ J g}^{-1} \text{ K}^{-1}$ (ref 56), the coupling constant can be calculated, provided C_{pc} is known. We utilized the two-scale-factor universality relation^{57,58}

$$C_{\text{pc}} = k_B X \alpha_0^{-1} \xi_0^{-3} \quad (34)$$

to derive C_{pc} from the amplitude, ξ_0 , of the fluctuation correlation length.

In eq 34, $X = 0.01966 \pm 0.00017$ according to renormalization group⁵⁹ and $X = 0.0188 \pm 0.00015$ according to series⁵⁸ calculations. With $\xi_0 = 0.23 \pm 0.02 \text{ nm}$, the amplitude $C_{\text{pc}} = (2.1 \pm 0.2) \times 10^5 \text{ J/(m}^3 \text{ K)}$ follows, corresponding to $C_{\text{pc}} = (0.264 \pm 0.2) \times 10^5 \text{ J/(g K)}$, if $\rho(T_c) = 0.7919 \times 10^3 \text{ kg m}^{-3}$ from ref 25 is used. This value is somewhat smaller but within the limits of error of $C_{\text{pc}} = 0.30 \pm 0.06 \text{ J/(g K)}$ from heat capacity measurements.⁶⁰ Using our C_{pc} value, the amount of the coupling constant results as $|g| = 0.26 \pm 0.05$ from eq 32.

The adiabatic coupling constant can be alternatively calculated as

$$g = \rho(T_c) C_p(T) \left(\frac{dT_c}{dP} - \frac{T\alpha_p}{\rho(T_c) C_p(T)} \right) \quad (35)$$

from the slope dT_c/dP in the pressure dependence of the critical temperature and the thermal expansion coefficient, α_p , at constant pressure. With $dT_c/dP = (0.37 \pm 0.05) \times 10^{12} \text{ (K m}^2\text{)/dyn}$,^{60,61} $\alpha_p = 1.22 \times 10^{-3} \text{ K}^{-1}$ (ref 27) or $\alpha_p = 1.34 \times 10^{-3} \text{ K}^{-1}$ (ref 56), with $C_p = 2.48 \text{ J/(g K)}$ ⁵⁶ close to T_c , and with the values of the other quantities as given above, $g = -0.29 \pm 0.04$ follows. The amount of this value is somewhat smaller than the amount of the coupling constant $g = 0.34 \pm 0.01$ determined previously from thermodynamic data,⁵⁶ but it agrees well with $|g| = 0.26 \pm 0.05$ derived from the amplitude of the ultrasonic spectra.

Conclusions. Shear viscosity, quasielastic light scattering, and ultrasonic attenuation data of the nitroethane/3-methylpentane mixture of critical composition can be consistently evaluated to yield the relaxation rate, Γ , of order parameter fluctuations and the scaling function, $F(\Omega)$, of the Bhattacharjee–Ferrell dynamic scaling theory. Not only close to the critical temperature but also in the crossover region, Γ from shear viscosity and light scattering measurements follows power law with the universal critical exponent. The amplitude $\Gamma_0 = 125 \times 10^9 \text{ s}^{-1}$ is almost as large as that of the similar system nitroethane/cyclohexane ($\Gamma_0 = 156 \times 10^9 \text{ s}^{-1}$), though the viscosities of both mixtures are substantially different. The relaxation rates from the shear viscosity and light scattering experiments also govern the frequency dependent acoustical attenuation coefficients. In addition, the scaling function data derived from these coefficients yield a scaled half-attenuation frequency of $\Omega_{1/2}^{\text{BF}} = 2.1$, as predicted by the Bhattacharjee–Ferrell theory. Using the two-scale-factor universality relation, the amplitude $\xi_0 = 0.23 \text{ nm}$ of the fluctuation correlation length can be used to calculate the amount, $|g|$, of the adiabatic coupling constant, g , from the amplitude in the sonic spectra $|g| = 0.29$ from another thermodynamic relation. Hence, the nitroethane/3-methylpentane mixture of critical composition obviously represents a suitable model system for the study of the critical behavior near the consolute point.

Acknowledgment. Dr. R. Behrends and Prof. S. Z. Mirzaev are thanked for their spirited discussions. Financial support by the Deutsche Forschungsgemeinschaft and the Volkswagen-Stiftung is gratefully acknowledged.

References and Notes

- (1) Anisimov, M. A. *Critical Phenomenon in Liquids and Liquid Crystals*; Gordon and Breach: London, 1991.
- (2) Binney, J. J.; Dowrick, N. J.; Fisher, A. J.; Newmann M. E. J. *The Theory of Critical Phenomena*; Clarendon: Oxford, U.K., 1992.
- (3) Stanley, H. E. *Rev. Mod. Phys.* **1999**, *71*, 388.

- (4) Onuki, A. *Phase Transition Dynamics*; Cambridge University Press: Cambridge, U.K., 2002.
- (5) Kadanoff, L. P.; Swift, J. *Phys. Rev.* **1968**, *166*, 89.
- (6) Halperin, B. I.; Hohenberg, P. C. *Phys. Rev.* **1969**, *177*, 952.
- (7) Ferrell, R. A. *Phys. Rev. Lett.* **1970**, *24*, 1169.
- (8) Hohenberg, P. C.; Halperin, B. I. *Rev. Mod. Phys.* **1977**, *49*, 435.
- (9) Bhattacharjee, J. K.; Ferrell, R. A. *Phys. Rev. A* **1981**, *24*, 1643.
- (10) Ferrell, R. A.; Bhattacharjee, J. K. *Phys. Rev. A* **1985**, *31*, 1788.
- (11) Bhattacharjee, J. K.; Ferrell, R. A. *Physica A* **1998**, *250*, 83.
- (12) Folk, R.; Moser, G. *Phys. Rev. E* **1998**, *57*, 705.
- (13) Folk, R.; Moser, G. *Phys. Rev. E* **1998**, *58*, 6246.
- (14) Folk, R.; Moser, G. *Int. J. Thermophys.* **1998**, *19*, 1003.
- (15) Onuki, A. *Phys. Rev. E* **1997**, *55*, 403.
- (16) Onuki, A. *J. Phys. Soc. Jpn.* **1997**, *66*, 511.
- (17) Kaatze, U.; Mirzaev, S. Z. *J. Phys. Chem. A* **2000**, *104*, 5430.
- (18) Telgmann, T.; Kaatze, U. *Langmuir* **2002**, *18*, 3068.
- (19) Schrader, W.; Halstenberg, S.; Behrends, R.; Kaatze, U. *J. Phys. Chem. B* **2003**, *107*, 14457.
- (20) Garland, C. W.; Sanchez, G. *J. Chem. Phys.* **1983**, *79*, 3090.
- (21) Harada, Y. Dynamics of Ordering Processes. In *Condensed Matter*; Komura, S., Furukawa, H., Eds.; Plenum: New York, 1988.
- (22) Behrends, R.; Iwanowski, I.; Kosmowska, M.; Szala, A.; Kaatze, U. *J. Chem. Phys.* **2004**, *121*, 5929.
- (23) Wims, A. M.; McIntyre, D.; Hynne, F. *J. Chem. Phys.* **1969**, *50*, 616.
- (24) Stein, A.; Allegra J. C.; Allen, G. F. *J. Chem. Phys.* **1971**, *55*, 4265.
- (25) Greer S. C.; Hocken, R. *J. Chem. Phys.* **1975**, *63*, 5067.
- (26) Chang, R. F. Burstyn, H.; Sengers, J. V. *Phys. Rev. A* **1979**, *19*, 866.
- (27) Tanaka, H.; Wada, Y. *Chem. Phys.* **1983**, *78*, 143.
- (28) Sørensen, C. M.; Mockler, R. C.; O'Sullivan, W. *Phys. Rev. A* **1977**, *16*, 365.
- (29) Nienwoudt, J. C.; Sengers, J. V. *J. Chem. Phys.* **1989**, *90*, 457.
- (30) Berg, R. F.; Moldover, M. R. *Phys. Rev. E* **1999**, *60*, 4079.
- (31) Chu, B. *Laser Light Scattering*; Academic: New York, 1991.
- (32) Dürr, U.; Mirzaev, S. Z.; Kaatze, U. *J. Phys. Chem. A* **2000**, *104*, 8855.
- (33) Schätzel, K. *Appl. Phys. B* **1987**, *42*, 193.
- (34) Schätzel, K.; Drewel, M.; Stimac, M. *Mod. Opt.* **1988**, *35*, 711.
- (35) Kaatze, U.; Behrends, R.; Lautscham, K. *Ultrasonics* **2001**, *39*, 393.
- (36) Eggers, F.; Kaatze, U.; Richmann, K. H.; Telgmann, T. *Meas. Sci. Technol.* **1994**, *5*, 1131.
- (37) Kaatze, U.; Kühnel, V.; Menzel, K.; Schwerdtfeger, S. *Meas. Sci. Technol.* **1993**, *4*, 1257.
- (38) Kaatze, U.; Lautscham, K.; Brai, M. *J. Phys. E: Sci. Instrum.* **1988**, *21*, 98.
- (39) Kaatze, U.; Lautscham, K. *J. Phys. E: Sci. Instrum.* **1986**, *19*, 1046.
- (40) Burstyn, H. C.; Sengers, J. V.; Esfandiari, P. *Phys. Rev. A* **1980**, *22*, 282.
- (41) Bhattacharjee, J. K.; Ferrell, R. A.; Basu, R. S.; Sengers, J. V. *Phys. Rev. A* **1981**, *24*, 1469.
- (42) Burstyn, H. C.; Sengers, J. V.; Bhattacharjee, J. K.; Ferrell, R. A. *Phys. Rev. A* **1983**, *28*, 1567.
- (43) Berg, R. F.; Moldover, M. R. *J. Chem. Phys.* **1988**, *89*, 3694.
- (44) Stokes, G. G. *Trans. Cambridge Philos. Soc.* **1845**, *8*, 287.
- (45) Einstein, A. *Ann. Phys.* **1905**, *17*, 549.
- (46) Kawasaki, K. *Ann. Phys. (N. Y.)* **1970**, *61*, 1.
- (47) Kawasaki, K. *Phys. Rev. A* **1970**, *1*, 1750.
- (48) Luetmer-Strathmann, J.; Sengers, J. V.; Olchoway, G. A. *J. Chem. Phys.* **1995**, *103*, 7482.
- (49) Calmettes, P. *Phys. Rev. Lett.* **1977**, *39*, 1151.
- (50) Matos Lopes, M. L. S.; Nieto de Castro, C. A.; Sengers, J. V. *Int. J. Thermophys.* **1992**, *13*, 283.
- (51) Behrends, R.; Kaatze, U.; Schach, M. *J. Chem. Phys.* **2003**, *119*, 7957.
- (52) Iwanowski, I.; Behrends, R.; Kaatze, U. *J. Chem. Phys.* **2004**, *120*, 9192.
- (53) Iwanowski, I.; Sattarow, A.; Behrends, R.; Mirzaev, S. Z.; Kaatze, U. *J. Chem. Phys.*, submitted for publication.
- (54) Mirzaev, S. Z.; Kaatze, U. *Phys. Rev. E* **2002**, *65*, 021509-1.
- (55) Behrends, R.; Kaatze, U. *Europhys. Lett.* **2004**, *65*, 221.
- (56) Clerke, E. A.; Sengers, J. V.; Ferrell, R. A.; Bhattacharjee, J. K. *Phys. Rev. A* **1983**, *27*, 2140.
- (57) Lui, A. J.; Fisher, M. E. *Physica A* **1989**, *156*, 35.
- (58) Rebillot, P. F.; Jacobs, D. T. *J. Chem. Phys.* **1998**, *109*, 4009.
- (59) Bervillier C.; Godrèche, C. *Phys. Rev. B* **1980**, *21*, 5427.
- (60) Sanchez, G.; Meichle, M.; Garland C. W. *Phys. Rev. A* **1983**, *28*, 1647.
- (61) Beysens, D.; Tufeu, R. *Rev. Phys. Appl.* **1979**, *14*, 907.